

The application of Bayesian change point detection in UAV fuel systems

Niculita, Ioan-Octavian; Skaf, Zakwan; Jennions, Ian K.

Published in:
Proceedings of the 3rd International Conference in Through-life Engineering Services

DOI:
[10.1016/j.procir.2014.07.119](https://doi.org/10.1016/j.procir.2014.07.119)

Publication date:
2014

Document Version
Publisher's PDF, also known as Version of record

[Link to publication in ResearchOnline](#)

Citation for published version (Harvard):
Niculita, I-O, Skaf, Z & Jennions, IK 2014, The application of Bayesian change point detection in UAV fuel systems. in *Proceedings of the 3rd International Conference in Through-life Engineering Services*. Procedia CIRP, Elsevier B.V., pp. 115-121, 3rd International Conference in Through-life Engineering Services, Cranfield, United Kingdom, 4/11/14. <https://doi.org/10.1016/j.procir.2014.07.119>

General rights

Copyright and moral rights for the publications made accessible in the public portal are retained by the authors and/or other copyright owners and it is a condition of accessing publications that users recognise and abide by the legal requirements associated with these rights.

Take down policy

If you believe that this document breaches copyright please view our takedown policy at <https://edshare.gcu.ac.uk/id/eprint/5179> for details of how to contact us.

3rd International Conference on Through-life Engineering Services

The Application of Bayesian Change Point Detection in UAV Fuel Systems

Octavian Niculita*, Zakwan Skaf, Ian K. Jennions

*IVHM Centre, Cranfield University, MK43 0AL, UK** Corresponding author. Tel.: +44 1234758394; E-mail address: o.niculita@cranfield.ac.uk

Abstract

A significant amount of research has been undertaken in statistics to develop and implement various change point detection techniques for different industrial applications. One of the successful change point detection techniques is Bayesian approach because of its strength to cope with uncertainties in the recorded data. The Bayesian Change Point (BCP) detection technique has the ability to overcome the uncertainty in estimating the number and location of change point due to its probabilistic theory. In this paper we implement the BCP detection technique to a laboratory based fuel rig system to detect the change in the pre-valve pressure signal due to a failure in the valve. The laboratory test-bed represents a Unmanned Aerial Vehicle (UAV) fuel system and its associated electrical power supply, control system and sensing capabilities. It is specifically designed in order to replicate a number of component degradation faults with high accuracy and repeatability so that it can produce benchmark datasets to demonstrate and assess the efficiency of the BCP algorithm. Simulation shows satisfactory results of implementing the proposed BCP approach. However, the computational complexity, and the high sensitivity due to the prior distribution on the number and location of the change points are the main disadvantages of the BCP approach

© 2014 The Authors. Published by Elsevier B.V. This is an open access article under the CC BY-NC-ND license

[\(http://creativecommons.org/licenses/by-nc-nd/3.0/\)](http://creativecommons.org/licenses/by-nc-nd/3.0/).

Peer-review under responsibility of the Programme Chair of the 3rd International Through-life Engineering Conference

Keywords: Fault detection, UAV fuel systems, Change points detection

1. Introduction

Change Point detection methods are used widely in industry to detect a change in parameter that result from unexpected operation condition. Bayesian Change Point (BCP) detection technique has been nominated as a power method in stochastic process for detecting the changes. In this paper, we aim to implement the BCP detection technique in the UAV fuel systems to demonstrate its efficiency.

The purpose of the fuel rig is to investigate fault detection and isolation, degradation, and state prediction in a representative system. The system has been modelled in different software packages used for the Integrated Vehicle Health Management (IVHM) system design. The test rig also has been used as a testing platform for novel signal processing techniques and algorithms that support IVHM

implementation. The hardware was built and will be used to validate predictions of diagnostic software packages, and also as a demonstrator to illustrate the performance of system damage detection and isolation techniques.

Running representative tests on any IVHM system is always problematic. To see any significant degradation requires running over a considerable period of time, cannot be easily reproduced, and is costly. Three different approaches could be taken. Firstly, accelerated testing; this could be achieved by increasing the duty of the components or by manufacturing them out of less durable materials. Secondly, by accurately knowing the degradation modes to be investigated, the components could be machined to represent the degraded mode. This only represents one snapshot in the wear process but could be repeated gradually increasing the effect. Simulation may be necessary to aid this process.

Thirdly, a different perspective could be taken: some degradation modes could be emulated, e.g. a filter replaced by a direct proportional valve so that a clogged filter failure mode could be simulated by gradually closing the valve. It is the latter approach that is adopted there.

2. Experimental setup

To make the development of the test rig manageable in a lab the fuel system was made representative of that of a small UAV engine (Figure 1). Adopting this approach allows the rig to be bench-top scale, minimizing cost whilst maximizing the aspects of the fuel system that can be investigated. The rig consists of the following representative components:

- Main and sump tanks
- External gear pump
- Filter
- Polyurethane tubing
- Solenoid shut off valve, direct proportional valves
- Non-return valve
- Control modules for pump, direct proportional valves and shut-off valve
- Instrumentation.

A connection between the drain valve of the sump tank and the refill valve of the main tank has been considered in order to realize a general reset of the test rig.

The following contrived components are also included in order to achieve safe operation in re-circulation and drain modes:

- A variable restrictor (ball valve) to simulate engine injection and to create back pressure when partially closed.
- A three way inlet/outlet valve to switch between recirculation and drain modes
- A drain tank and valves so that the main tank can be drained

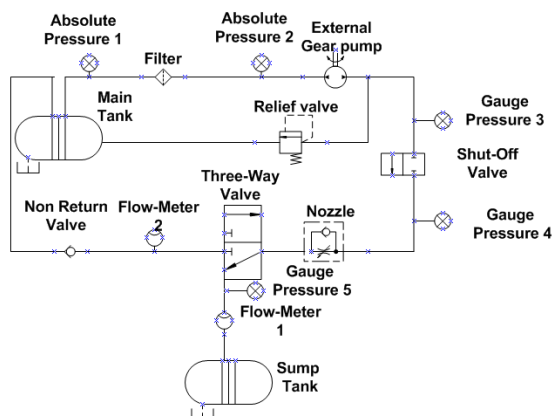


Fig. 1. Schematic of the experimental setup.

The relief valve shown in Figure 1 was not incorporated into the final system as the gear pump features its own relief valve. The realization of the above system is shown in Figure 2.

In order to control and acquire data from the fuel system test rig, a system using National Instruments LabVIEW virtual instrumentation has been utilized: a CDAQ – 9172 device with six compact DAQ modules: NI 9485, NI 9205, NI 9472, NI 9401 and two NI 9263.

The National Instruments (NI) 9485 is a 8-channel solid-state relay sourcing or sinking digital output module for any CompactDAQ or CompactRIO chassis. One channel was used to provide access to a solid-state relay for switching the 24V voltage applied to the shut-off valve in order to control the open/close position. The NI 9205 module receives the analogue voltage output from the pressure transducers and flow-meters, converts this information using the pre-defined calibration curves into digitized information readable on the GUI. The NI 9472 module is a 8-channel 24V logic, sourcing digital output module which provides the signals to the pump inverter in order to implement the pump controls (Start pump, Stop pump, Increase speed, De-crease speed, Forward/Reverse, Relative Speed). The NI 9401 module counts the rotational speed laser sensor analogue output pulses and converts them into frequency for calculation of the pump speed. The NI 9263 module is a 4-channel, 100 kS/s simultaneously updating analog output module which enables the implementation of the direct proportional valves position control. Valve position is modified by varying the voltage applied to the solenoid.



Fig. 2. Fuel system test rig.

The main GUI is shown in Figure 3. The user has control over shut-off valve position, pump speed (manual or mission profile mode) and direct proportional valves position. Within the same GUI the sensor output for rotational speed is displayed, pressure in different points of the fuel rig and volumetric flow rate on both re-circulation line and engine feed line. National Instruments LabVIEW software version 2014 was used to customize the control for the entire system. Referring to Figure 3 the controls are structured in three layers (top three layers) of the GUI:

- The top layer contains Pump Control Unit and Valve Control Unit.
- The second layer enables the control of the fault injection mechanisms at the component level. This is

done via knobs that are setting the position of five Direct Proportional Valves (DPVs).

- The third layer allows control of fault injection mechanism at the sensor level.

The data presented to the user in the GUI on the bottom layer: pressures in different points of the system (e.g. before filter, after filter, after pump, after shut-off valve, before sump tank) on the left hand side; volumetric flow rate in the main line on the right hand side of this layer.

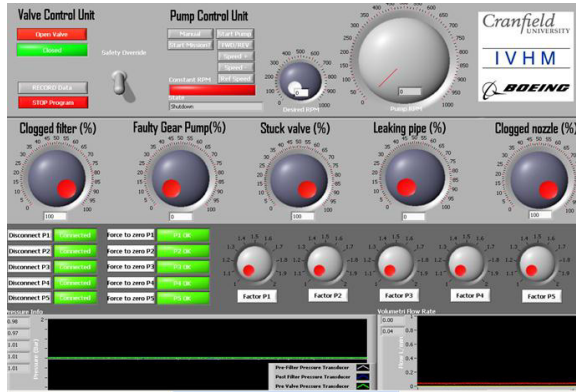


Fig. 3. Fuel system – GUI for controls

3. System behavior under healthy and faulty conditions

From the hardware and software point of view, the control system accommodates five failure modes in a plug and play manner: a clogged filter, a degraded pump, a stuck valve, a leaking pipe and a clogged nozzle. Physical behavior of the fuel system affected by these failure modes under different degrees of severity is depicted in Figures 4-8. Volumetric flow rate drops in all cases, therefore the following figures only capture the pressure at five different locations (pressure across the filter, pressure across the shut-off valve and pressure after the nozzle). P1 is the pressure measured before the filter, P2 represents the pressure after the filter, P3 and P4 are the pressure values measured before and after the shut-off valve and P5 is the pressure measured before the sump tank. The degradation phenomenon for each individual type of fault was physically implemented on the test rig using DPVs. The filter was replaced by a DPV and set to be initially fully open (this setup captures the healthy scenario as the pressure drop across the valve was identical to the pressure drop across the filter). By gradually closing this valve the system replicates a behavior of a clogged filter (Figure 4). The degraded pump was emulated through a leak after the pump. The severity of the leak was controlled by adding another DPV in the system which is controlling the level of flow that is released outside the main line. Initially this valve was full closed; the behavior of the system when valve is open (5-100%) is depicted in Figure 5. The failure of the shut-off valve (being stuck in amid range position) was implemented by adding in line another DPV. Different degrees of severity of the seizure of the shut-off valve can be obtained by gradually closing this valve

(initially set to be fully open). Its effects on pressure measurements are highlighted in Figure 6. The leaking pipe failure mode was emulated through a leak in the pipe connecting the shut-off valve and the nozzle. The severity of the leak was controlled by adding another DPV in the system which is controlling the level of flow that is released outside the main line. Initially this valve was full closed; the behavior of the system when valve is open (between 5 and 100%) is depicted in Figure 7. Due to dirty fuel, the nozzle component can get clogged. This phenomenon was emulated on the test rig by replacing the nozzle with a DPV. Its effects on system behavior are captured in Figure 8.

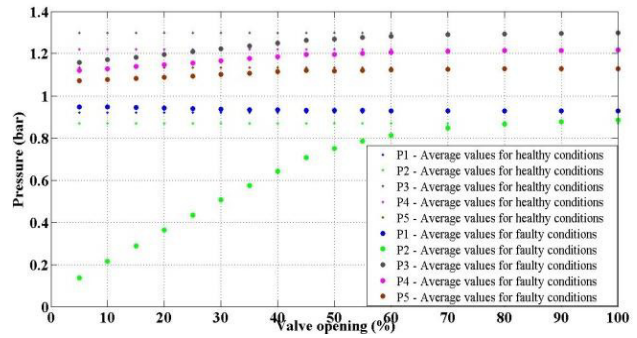


Fig. 4. Physical behavior – Clogged filter scenario

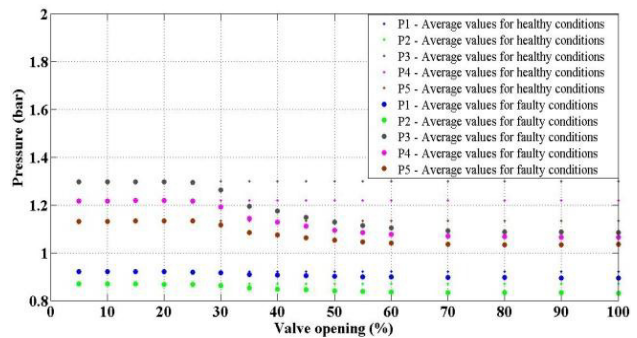


Fig. 5. Physical behavior – Degraded pump scenario

The points in Figures 4-8 represent the average values of 1min of data for each individual pressure measurement (sampled at 1kHz). The real data for each individual faulty scenario for different degrees of severity was discussed in [1], [2].

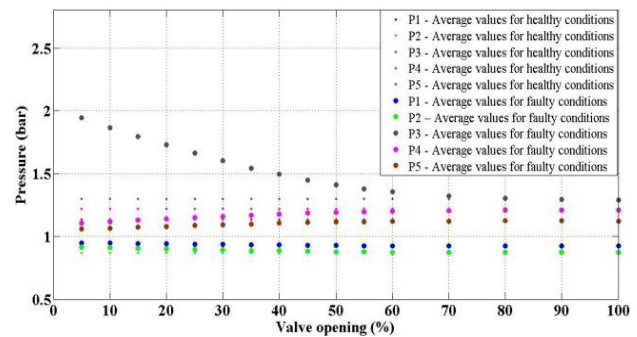


Fig. 6. Physical behavior – Stuck valve scenario

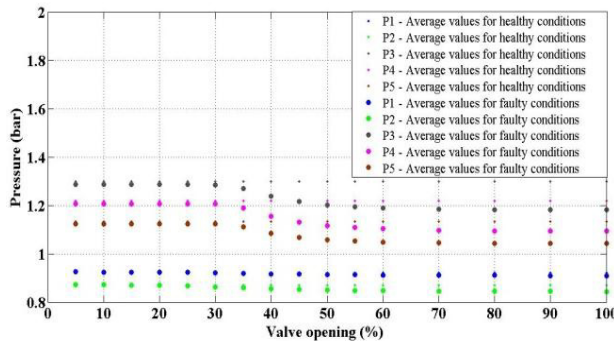


Fig. 7. Physical behavior – Leaking pipe scenario

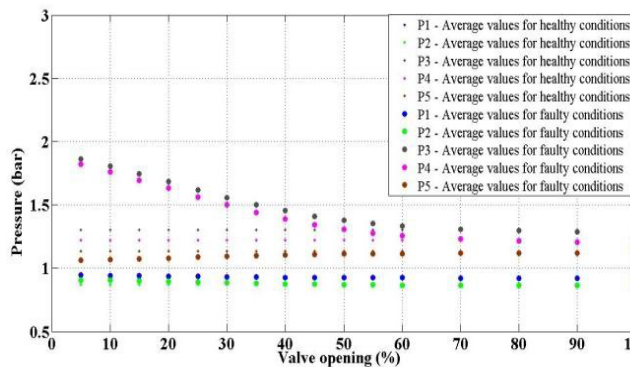


Fig. 8. Physical behavior – Clogged nozzle scenario

4. Change Point Detection

A significant amount of research in the statistics community has been undertaken to develop the change point detection methods for the abrupt changes in data over the last three decades [3, 4, 5, 6]. Change-point detection problem has been significantly developed and used in various applications, such as signal segmentation of a data stream [7], fraud detection in mobile networks [8], climate change detection [9], motion detection in vision systems [10], stock market prices [11], nuclear engineering [12], and the aerospace domain [13, 14].

Most of the recent research in change-point detection adopts the Bayesian approach (see, for example, [13, 14]) which allows direct probability statements about unknown quantities, as opposed to weaker confidence statements about them. The BCP detection technique is a powerful method comparing with the existing change point detection approaches due to its accuracy and effectiveness. A significant amount of publication can be found in the literature review on the BCP detection approaches [15, 16, 17, 18, 19, 18]. The Bayesian approach to multiple change-points dates back to the seminal paper of [21]. [22] extended the model in [23] of normal mean shift to Gaussian autoregressive models with unexpected

changes in the value and variance, by approximating the posterior distribution using the Gibbs sampler.

Most of the proposed BCP approaches in the literature review are retrospective [26], and have demonstrated strong performance for off-line datasets. Recently, a new online BCP detection technique was recently presented by [19], and in an alternative formulation by [27]. While computational cost can be made to be approximately linear in [27] by applying resampling strategies, a preferred recursive formulation by [19] provides a closed form solution that is linear and introduces no approximation errors.

The objective in this research is to implement the new developed BCP detection, suggested recently by [17]. This method makes use of the Bayesian approach. As such, it is suitable for the analysis and understanding of time series data. The results will demonstrate the effectiveness of this method in the UAF fuel system.

5. Description of the algorithm

In this section, the developed BCP detection algorithm in [17] will be used to detect the change in the pre-valve pressure signal. We describe briefly the model and the required prior distributions, and how these are used to perfectly sample from the posterior probabilities of given points being change points. More details about the BCP can be found in [17].

Let Y and m denote the dependent variable and predictor variables, respectively. Then, the linear regression of X_1, \dots, X_m , can be presented by Equation (1) as follows:

$$Y = \sum_{l=1}^m \beta_l X_l + \varepsilon \quad (1)$$

where β_l and ε present the l th regression coefficient and the random error term, respectively. The goal of this algorithm is to build a piecewise regression model whose regime boundaries are the change in the recorded data.

Let $X = [X_1, X_2, \dots, X_m]$ be the matrix of predictor variables, $Y = [Y_1, Y_2, \dots, Y_n]$ be the vector of response variable, N be the total number of data points, σ^2 be the residual variance, and $\{C\}$ be the set of change points whose location are $c_0 = 0, c_1, c_2, \dots, c_k, c_{k+1} = N$.

The main steps of the BCP algorithm are detailed below:

5.1. Calculating $f(Y_{i,j} | X_{i,j})$:

Denote $X = [X_1, X_2, \dots, X_m]$ the repressors in the regression model, and the error ε is mean zero, and normally distributed.

The probability density of the data, $f(Y_{i,j} | X_{i,j})$, can be calculated as follows [17]:

$$f(Y_{i,j}|X_{i,j}) = \frac{(\nu_0 \sigma_0^2 / 2)^{\nu_0/2} \Gamma(\nu_n / 2) (k_0)^{n/2}}{\Gamma(\nu_0 / 2) (s_n)^{\nu_n/2} (2\pi)^{n/2} |X_{i,j}^T X_{i,j} + k_0 I|^{1/2}} \quad (2)$$

where $\nu_n = \nu_0 + n$, $\beta^* = (X_{i,j}^T X_{i,j} + k_0 I)^{-1} X_{i,j}^T Y_{i,j}$, $s_n = (Y_{i,j} - X_{i,j} \beta^*)^T (Y_{i,j} - X_{i,j} \beta^*) + k_0 \beta^{*T} \beta^* + \nu_0 \sigma_0^2$, β a multivariate normal, $\beta \sim N(0, \sigma^2 / k_0)$, $\sigma^2 \sim \text{Scaled-Inversed } X^2(\nu_0, \sigma_0^2)$, ν_0 and σ_0^2 act as pseudo data points, I is the identity matrix, k_0 is a scale parameter, Γ is the gamma function, and n to be the number of samplings points in a substring. More details about the derivation of Eq. 2 can be found in [17]:

5.2. Forward recursion

Denote $Y = [Y_1, Y_2, \dots, Y_j]$ has k change points and its density is $P_k(Y_{1:j})$. Then, $P_k(Y_{1:j})$ can be calculated recursively as follows [17]:

$$P_1(Y_{1:j}) = \sum_{v < j} f(Y_{1:v}) f(Y_{v+1:j}) \quad (3)$$

$$P_k(Y_{1:j}) = \sum_{v < j} P_{k-1}(Y_{1:v}) f(Y_{v+1:j}) \quad (4)$$

for $j = 1, 2, \dots, N$

5.3. Stochastic back trace via Bayes rule

Defining the prior distribution on the number and location of the of change points ($f(K=k)$ and $f(c_1, c_2, \dots, c_k | K=k)$) are essentially to calculating the partition functions as follows [17]:

$$f(Y_{1:N}) = \sum_{k=0}^{K_{\max}} \sum_{c_1, \dots, c_k} f(Y_{1:N} | K=k, c_1, \dots, c_k) \times f(K=k, c_1, \dots, c_k) \quad (5)$$

and

$$f(K=k, c_1, \dots, c_k) = \frac{0.5}{\left(k_{\max} \binom{N}{k} \right)}$$

where k_{\max} denote the maximum number of changes in the data.

6. Experiment & Results

Our aim in this section is to detect the change in the pre-valve pressure signal in the UAV fuel system due to a failure of valve being jammed in a mid-range position. To detect these changes in the pre-valve pressure signal, we use the BCP detection technique developed by [17]. The malfunction of the

shut-off valve is implemented for different degrees of severity of the seizure of the shut-off valve by using the DPV. Nine degrees of severity were generated corresponding to 100%, 90%, 80%, 70%, 60%, 50%, 40%, 30% and 20% valve opening. Position 100% valve open corresponds to a healthy valve, 20% shut-off valve open corresponds to an almost stuck shut-off valve. The fault is injected for 30sec before removing it completely (back to health shut-off valve) and injecting it again with different degree of severity.

The threshold value of the flow rate through the shut-off valve is the most important detection setting for making decision about a significant fault in the valve. When the change in the pre-valve pressure signal detects due to a failure in the valve and the flow rate decreases we compare the current flow rate with the threshold. If more flow rate than defined by threshold has changed we assume that we have detected a fault in the valve.

In this work, we assumed the minimum accepted level for the volumetric flow rate through the valve to be 0.66 l/min (Figure 9). When the probability of change point in the pre-valve pressure signal is more than 0.95 and the flow rate less than 0.66 l/min, we can confirm that a fault in the valve is detected. Setting the threshold value is a big challenge, because the sensitivity of change detection will be decreased if the value of the threshold is set too high. In contrast, if the value of the threshold is set too low, this will increase the ratio of the false alarm rate.

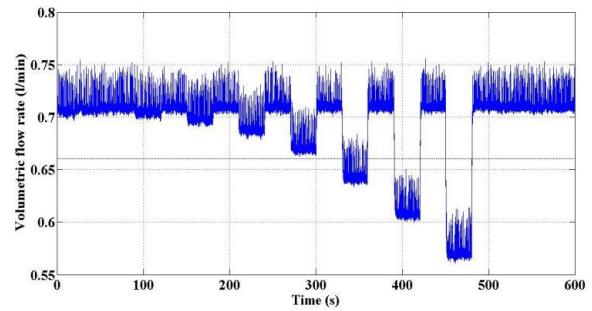


Fig. 9 Stuck valve scenario – volumetric flow rate and the threshold between healthy and faulty conditions

The data for each individual pressure measurement is recorded for 600 sec. 2400 samples of data ($N=2400$) were recorded for testing. 10 datasets has been used for testing. We assumed that the pre-valve pressure regime between each change can be presented linearly by $Y = \beta_1 + \beta_2 X$, and set the maximum number of changes (in the pre-valve pressure to $k_{\max} = 50$. We set the value of ν_0 , σ_0^2 , and k_0 to be 0.1, 0.04, and 0.013, respectively.

The analysis of the pressure transducer (measure before the shut-off valve) by the BCP approach is shown in Figure 10. The blue (solid) line represents the Pre-Valve pressure signal, while the dashed blue line represents the model of the Pre-

Valve pressure signal predicted by the BCP algorithm and the red line represents the probability of a change point in the Pre-Valve pressure signal due to a failure in the valve.

The values of the probability of detecting a change in the pressure signal are shown as spikes at the bottom of Figure 10. The shape of the spikes presents the confidence in detecting the change and the uncertainty in the exact time of detecting the change in the pressure signal. For example, spike with small amplitude and wide spread indicates low confidence in detecting the change and wide range of uncertainty about the exact time of detecting the change in the signal, and vice versa.

As shown in Figure 10, there are some spikes with probability of change more than 0.95 which indicate a change in the shut-off valve, but this change will be ignored because the flow rate at the change point is less than 0.66 l/min. For example, the probability of change when emulate severity with 50% valve opening is 0.99 and the flow rate at that point through the valve is around 0.68 l/min. On the other hand, when the probability of change is more than 0.95 and the flow rate at the change point is more than 0.66 l/min a serious change will be detected and confirmed, such as the probability of change when emulate severity with 50% valve opening is 0.99 and the flow rate at that point is around 0.60 l/min.

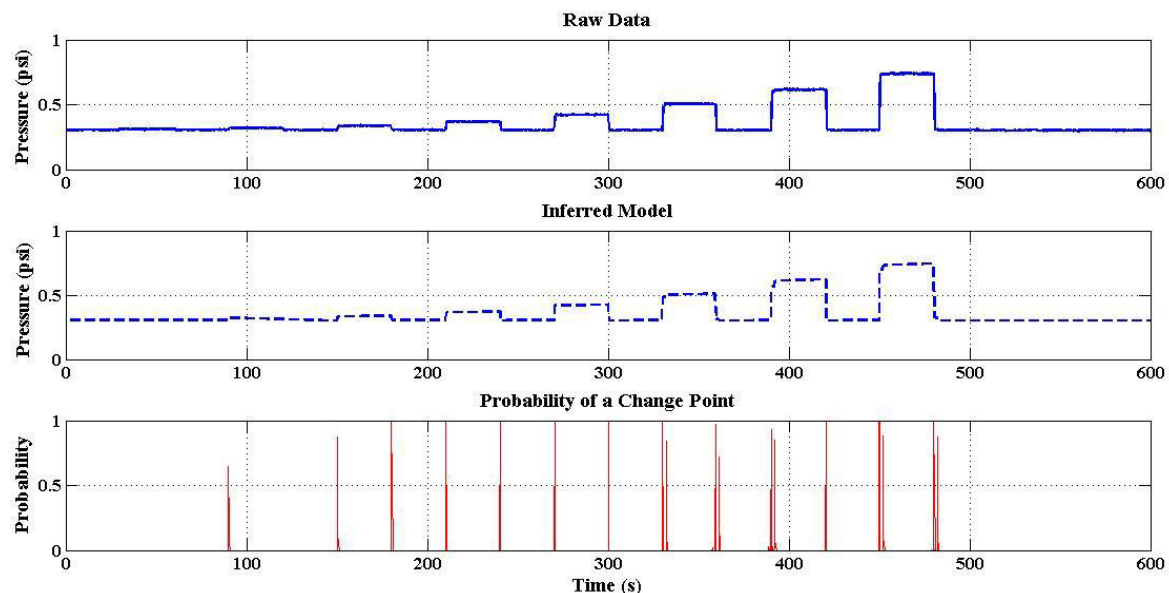
The BCP approach is tested with different ν_0 , σ_0 , and k_0 values. It was clear that the value of these parameters which

BCP because it has big impact on the posterior distribution of the number of detected changes in the pressure signal. Also, it was noticed that noise amplitude has big impact on the shape of the spikes. For example, increasing the amplitude of the pressure signal will increase the spread of the spike which indicates more uncertainty about the exact time of detecting the change in the pressure signal, and vice versa.

7. Conclusions

A linear regression model used to construct the Pre-Valve pressure signal. The number and location of serious changes in the valve was identified through implementing the BCP detection algorithm to the Pre-Valve pressure signal. The conclusion about the fault severity of a stuck shut-off valve was drawn by correlating the probability of change point in the pressure signal with the required flow rate through the valve. The level of noise in the pressure signal had big impact of changing the spread of the spikes and consequently changing the level of confidence in defining the time of change in the pressure signal.

A significant advantage of using the BCP approach in this work is its ability to cope with the uncertainty surrounding the solution regarding the number and location of change points in the Pre-Valve pressure signal due to a failure in the valve. However, the computational complexity, and the high sensitivity due to the prior distribution on the number and location of the change points are the main disadvantages of the BCP approach.



define the prior distribution is

Fig 10: Raw data and inferred model with change point locations indicated

References

- [1] Niculita O., Jennions, I.K., Irving P. (2013). Design for diagnostic and prognostics: A physical-functional approach, IEEE Aeroconf, BigSky Montana, DOI: 10.1109/AERO.2013.6497143
- [2] Niculita, O., Irving, P., and Jennions, I. K. (2012). Use of COTS Functional Analysis Software as an IVHM Design Tool for Detection and Isolation of UAV Fuel System Faults. In Proceedings of the Prognostic and Health Management Society Conference.
- [3] Basseville, M., & Nikiforov, I. V. (1993). Detection of abrupt changes: theory and application. Upper Saddle River, NJ, USA: Prentice-Hall, Inc.
- [4] Brodsky, B. E., & Darkhovsky, B. S. (1993). Nonparametric Methods in Change-point Problems. Dordrecht: Kluwer.
- [5] Gustafsson, F. (2000). Adaptive Filtering and Change Detection. Wiley.
- [6] Kawahara, Y., & Sugiyama, M. (2012). Sequential changepoint detection based on direct density-ratio estimation. Stat. Anal. Data Min., 5(2), 114–127.
- [7] Tobon-Mejia, D., Medjaher, K., Zerhouni, N., & Tripot, G. (2011). Hidden markov models for failure diagnostic and prognostic. In Prognostics and system health management conference (phm-shenzhen), 2011 (p. 1 -8).
- [8] Bolton, R. J., & Hand, D. J. (2002). Statistical fraud detection: A review. Statistical Science, 17, 2002.
- [9] Reeves, J., Chen, J., Wang, X. L., Lund, R., & QiQi, L. (2007). A review and comparison of changepoint detection techniques for climate data. Journal of Applied Meteorology and Climatology, 46(6), 900–915.
- [10] Ke, Y., Sukthankar, R., & Hebert, M. (2007). Event detection in crowded videos. In IEEE international conference on computer vision.
- [11] Chen, J., & Gupta, A. K. (1997). Testing and locating variance changepoints with application to stock prices. Journal of the American Statistical Association, 92(438), 739–747.
- [12] Fearnhead, P., & Clifford, P. (2003). On-Line Inference for Hidden Markov Models via Particle Filters. Journal of the Royal Statistical Society. Series B (Statistical Methodology), 65(4), 887–899.
- [13] Fujimaki, R. (2005). An approach to spacecraft anomaly detection problem using kernel feature space. In Proceedings pakdd-2005: Ninth pacific-asia conference on knowledge discovery and data mining. ACM Press.
- [14] Skaf, Z., Zaidan, M.A., Harrison, R.F., and Mills. A.R. (2013). Accommodating repair actions into gas turbine prognostics. In Annual conference of the prognostics and health management society 2013.
- [15] Turner, R., Saatci, Y., & Rasmussen, C. E. (2009). Adaptive sequential Bayesian change point detection.
- [16] Wilson, R. C., Nassar, M. R., & Gold, J. I. (2010). Bayesian online learning of the hazard rate in change-point problems. Neural computation, 22(9), 2452–2476.
- [17] Ruggieri, E. (2013). A Bayesian approach to detecting change points in climatic records. Int. J. Climatol., 33(2), 520–528.
- [18] Chowdhury, M. F., Selouani, S., & O'Shaughnessy, D. (2012). Bayesian on-line spectral change point detection: a soft computing approach for on-line asr. Int. J. Speech Technol., 15(1), 5–23.
- [19] Adams, R. P., & MacKay, D. J. (2007). Bayesian online changepoint detection. arXiv preprint arXiv:0710.3742.
- [20] Barry, D., & Hartigan, J. A. (1993). A bayesian analysis for change point problems. Journal of the American Statistical Association, 88(421), 309–319.
- [21] Chernoff, H. and Zacks, S. (1964). Estimating the current mean of a Normal distribution which is subject to changes in time. Ann. Statist. 35, 999-1018.
- [22] McCulloch, R. E. and Tsay, R. S. (1993). Bayesian inference and prediction for mean and variance shifts in autoregressive time series. J. Amer. Statist. Assoc. 88, 968-978.
- [23] Perreault, L., M. Hache, M. Slivitzky, and B. Bobee, (1999): Detection of changes in precipitation and runoff over eastern Canada and U.S. using Bayesian approach. Stochastic Environ. Res. Risk Assess., 13, 201–216.
- [24] Perreault, L., E. Parent, J. Bernier, B. Bobee, and M. Slivitzky, (2000). Retrospective multivariate Bayesian change-point analysis: A simultaneous single change in the mean of several hydrological sequences. Stochastic Environ. Res. Risk Assess., 14, 243–261.
- [25] Seidou, O., and T. Ouara, (2007). Recursion-based multiple change point detection in multiple linear regression and application to river streamflows. Water Resour. Res., 43, W07404, doi:10.1029/2006WR005021.
- [26] Xuan, X., & Murphy, K. (2007). Modeling changing dependency structure in multivariate time series. In Proceedings international conference in machine learning.
- [27] Fearnhead, P., & Liu, Z. (2007). On-line inference for multiple change points problems. Journal of the Royal Statistical Society B, 69, 589–605.